CHALMERS

Evaluation of Symbol Timing Recovery Algorithms in a High-Speed Fiber-Optic Communication System

Master's Thesis in Integrated Electronic System Design

Pavithra Muralidharan

Chalmers University of Technology
Department of Computer Science and Engineering
Gothenburg, Sweden, 2012

Evaluation of Symbol Timing Recovery Algorithms in a High-Speed Fiber-Optic Communication System

Pavithra Muralidharan

Examiner: Per Larsson-Edefors

Chalmers University of Technology
Department of Computer Science and Engineering
Gothenburg, Sweden, 2012
SE-412 96 Gothenburg Sweden
Telephone + 46 (0)31-772 1000

Abstract

In high speed fiber optical communication system, symbol synchronization plays a key role. The received signal with timing offset will degrade the performance of symbol synchronization. It is, therefore, important to estimate this timing offset and perform synchronization based on the estimation. Symbol synchronization can be performed by feedforward and feedback algorithms.

In this thesis Maximum likelihood, Oerder and Meyr, Gardner symbol timing recovery (STR) algorithms are evaluated for fiber optic communiciation system. Three master thesis students are involved in this project. Ai Yun developed STR algorithms, Evaluation of STR were performed by Pavithra Muralidharan and Hardware implementation by Tauseef Ahmad. This thesis report describes the evaluation of STR algorithm in detail.

A test bench set up was developed in MATLAB to model optical communication system, and this set up was used for evaluation. Modeled channel impairments were used to analyze their effect on symbol timing recovery. Alongside an estimate of chromatic dispersion filters are also provided.

Though performance differences of the three algorithms were marginal, when they are modified for hardware, it was found that Gardner will be an area efficient algorithm and Oerder and Meyr algorithm will be efficient in terms of power. As a result of this evaluation and hardware implementation Oerder and Meyr algorithm is a better choice in terms of area, power and performance.

Acknowledgements

My Sincere thanks to Per Larsson-Edefors, Lars Svensson(CSE),Magnus Karlsson, Pontus Johanisson(MC2),Erik Agrell, Henk Wymeersch, Naga VishnuKanth Irukulapati (S2), for their kind support and valuable comments

Pavithra Muralidharan, Gothenburg

Contents

List of Figures

Nomenclature

A/D	Analog to Digital
AAF	Anti-Aliasing Filter
ASIC	Application Specific Integrated Circuit
BER	Bit Error Rate
BUT	Block Under Test
CD	Chromatic Dispersion
FB	Feedback
FF	Feedforward
FPGA	Field Programmable Gate Array
GBaud	Giga Baud
IFT	Inverse Fourier Transform
ISI	Inter Symbol Interference
ML	Maximum Likelihood
ML	Maximum likelihood
OM	Oerder & Meyr
PMD	Polarization Mode Dispersion
QAM	Quadrature Amplitude Modulation
RZ	Return to Zero
STR	Symbol Timing Recovery

1

Introduction

In communication systems, carrier synchronization, symbol synchronization and phase synchronization must be performed at the receiver for the proper reception of the transmitted signal. The performance of these synchronizers directly affects the performance of the receiver. The better the synchronization, the better the results of the receiver. In this project, we developed three different algorithms for symbol timing recovery [1], evaluated them in a optical communication environment and implemented the algorithms in hardware [2]. This thesis focuses on the evaluation of different algorithms in the presence of channel impairments, and the effort needed to set up the MATLAB environment used for evaluation.

Optical communication systems have the capacity to deliver higher data rates than, for example, wireless systems. Unlike wireless communication, which would need very complex modulation formats to achieve high data rates, optical communication system has the ability to achieve high data rates using relatively simple modulation formats. Thus, initially ON-OFF keying was used in optical communication to transmit data [3].

However, today's growing demand for even higher data rates requires optical communication systems to have highly complex modulation formats. At very high data rates, the transmitted symbols suffer significantly from channel impairments, which must be compensated digitally in the receiver side. Digital compensation seems to be cost effective compared to optical compensations [4].

Among the various hardware platforms available, FPGAs (Field Programmable Gate Arrays) were initially chosen for this project, as vehicle of hardware implementation evaluation. FPGAs consist of matrix of configurable logic block linked by a reprogrammable interconnection network [5] and are considered flexible due to their reprogrammable property. Besides reprogrammability, FPGAs have a relatively limited time to market and NRE (Non-Recurring Engineering) cost compared to ASICs (Application Specific Integrated circuits).

In this project, symbol timing recovery (STR) algorithms will be implemented in hardware for a 112-Gbits/sec system. It was found, during the early stages of implementation, that the FPGA has severe limitations with I/O pins for this application. This led us to the choice of ASIC as implementation target. ASICs posses a huge potential for exploiting parallelism and performing efficient computation, in terms of using less power and area compared to FPGAs [6]. However, ASICs are application specific and, thus, the maximal performance is obtained at the expense of high NRE costs. Furthermore, an ASIC is not reprogrammable and hence it cannot be upgraded.

In this report, Chapter 2 describes the modeling of the channel impairments and the evaluation setup. Chapter 3 describes the various STR algorithms, while Chapter 4 discusses the performance and trade-offs of different algorithms in terms of performance, area and power. Chapter 5 provides a conclusion and discusses future work of this project.

1.1 Problem Description

This project relates the algorithm development with hardware cost, complexity, area and power. The various blocks available in the receiver of an optical communication system are chromatic dispersion (CD) filters, symbol timing recovery, equalizer, etc. Focus is put on one particular block of interest in the receiver, and in a step by step approach, implementation and analysis are performed. Owing to the availability of different algorithms for symbol timing recovery (STR), the STR block was chosen in this project. Previously, equalizers used for the compensation of Polarization Mode Dispersion (PMD), and residual CD were implemented in hardware [7].

Symbol timing recovery involves the estimation of the symbol period, which is a known quantity but due to oscillator drift, symbol timing will deviate from the known value. The timing offset needs to be estimated before the symbol recovery. Figure 2.1 shows the sampling done at known sampling frequency (1/Ts), however, due to drift in timing the symbols are not present at the known sampling frequency. The objective of the symbol timing recovery is to estimate the timing offset (τ) and to compensate for the offset. The offset can be estimated using both feedforward and feedback algorithms. In order to analyze pros and cons of both techniques, two feedforward algorithms and one feedback algorithm are to be developed and evaluated.

Since the focus of the project is mainly on STR for fiber optic communication system, the STR algorithms must be robust to fiber optical channel impairments. To test the robustness of these algorithms an evaluation setup was required. The evaluation setup is a MATLAB simulation setup that contain transmitter, optical channel and receiver.

The evaluation setup must be able to introduce optical channel impairments and allow the designer to analyze the impact of the STR algorithm on the performance. Also, it should be possible to model and evaluate the impact of optical channel impairments on performance.

After verifying the robustness of the STR algorithms for optical channel impairments, it is necessary to compare the cost of these algorithms for the hardware area and power consumption. Implementation of these algorithms in hardware will give the area and power estimates of different algorithms.

In short, the project begins with the development of algorithms, followed by evaluating them and finally by the hardware implementation of these algorithms. These three major parts are done by three master thesis students (see figure 1.2).

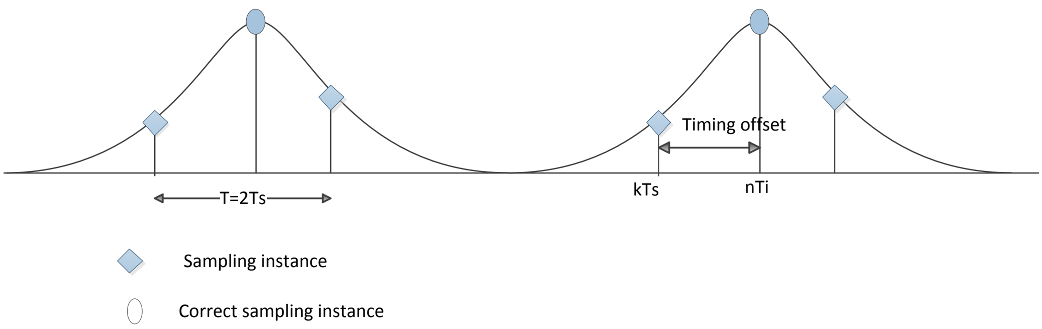

Figure 1.1: Sampling

- kT_s-Initial sampling instance.
- τT_s- Timing offset.
- nT_i-Final sampling instance.
- $nT_i = kT_s + \tau T_s$.

This project is done by three master students, with supervision from professors from the CSE, MC2, and S2 departments of Chalmers University. The flow chart in figure 1.2 shows the work flow between the three students involved in this project.

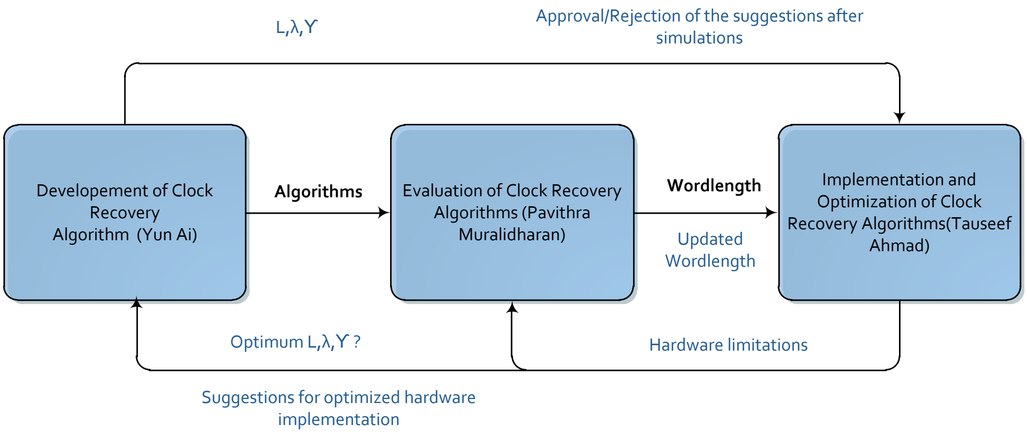

Figure 1.2: Work Flow.

2

Evaluation Setup

The block diagram of a evaluation setup—also called a system test bench—developed in MATLAB to represent the optical communication system is shown in figure 2.1. This test bench is used for the evaluation of symbol timing recovery (STR) algorithms. The highlighted block in figure 2.1 is the block of interest. This STR block will be represented using different algorithms, whose performance will be evaluated in the presence of various optical channel impairments. The bit error rate (BER) and the timing estimation error are the metrics used for evaluating performance. Overall, the versatility of the test bench allows for exploration into the impact of optical channel impairments on different STR algorithms and their implementations.

Using the test bench to ascertain, for example, data resolution in terms of word lengths, three different STR algorithms are developed [1] and implemented in hardware [2]. The word length estimation procedure is important as it impacts not only the BER, but also hardware parameters such as area and power consumption. The established word lengths are used for hardware implementation.

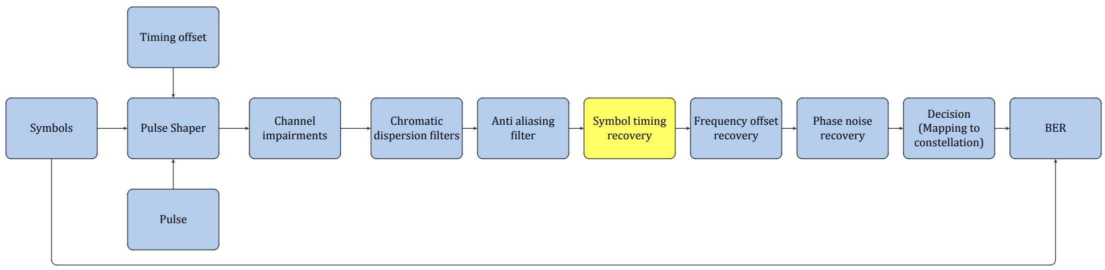

Figure 2.1: Evaluation setup using a test bench in MATLAB.

2.1 Transmitter

The system modeled in the test bench consists of a transmitter, channel and receiver. In this project, a modulator, a pulse generator and a pulse shaper would constitute the transmitter. The block diagram of the transmitter is shown in figure 2.2. Pseudo random symbols are generated and modulated in the modulator. The pulse generator will generate Gaussian pulses; specifically RZ (Return to Zero) pulses, which tend to have good tolerance to nonlinearities [8], with different duty cycles. RZ pulses with duty cycles of 30%, 50 % and 67% are supported in this test bench.

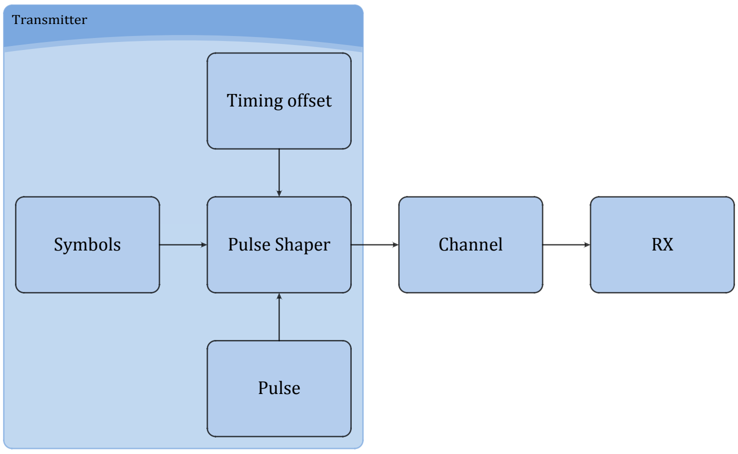

Figure 2.2: Transmitter.

$$E_{33}(t) = \begin{cases} \frac{1}{\sqrt{E_{33}}} sin(\frac{\pi}{2}\left[1 + sin\frac{\pi t}{T_s}\right]), & \text{for} \frac{-T_s}{2} \leq t \leq \frac{-T_s}{2} \\ 0, & \text{Otherwise} \end{cases} \tag{2.1}$$

$$E_{50}(t) = \begin{cases} \frac{1}{\sqrt{E_{50}}} sin(\frac{\pi}{4}\left[1 + cos\frac{2\pi t}{T_s}\right]), & \text{for} \frac{-T_s}{2} \leq t \leq \frac{-T_s}{2} \\ 0, & \text{Otherwise} \end{cases} \tag{2.2}$$

$$E_{67}(t) = \begin{cases} \frac{1}{\sqrt{E_{67}}} sin(\frac{\pi}{2} cos\frac{\pi t}{T_s}), & \text{for} \frac{-T_s}{2} \leq t \leq \frac{-T_s}{2} \\ 0, & \text{Otherwise} \end{cases} \tag{2.3}$$

In an optical system, the RZ pulses are generated using Mach Zehnder modulators. The process of generation of optical pulse by this modulator is not discussed here, but instead the function used to model the RZ pulses is given by equations (2.1)-(2.3). An RZ pulse with different duty cycles is shown in figure 2.3. Pulse shapes with different duty cycles were used to observe the effect of pulse and account for bandwidth of the optical system.

For instance, the pulse with 33% duty cycle is the shortest pulse in the time domain, but the frequency spectrum is broader compared to the 67% duty cycle pulse. In this thesis, simulations were performed using 67% duty cycle pulses.

The next block in this setup is the pulse shaper. The main purpose of pulse shaping is to make an efficient use of bandwidth and reduce inter symbol interference (ISI).

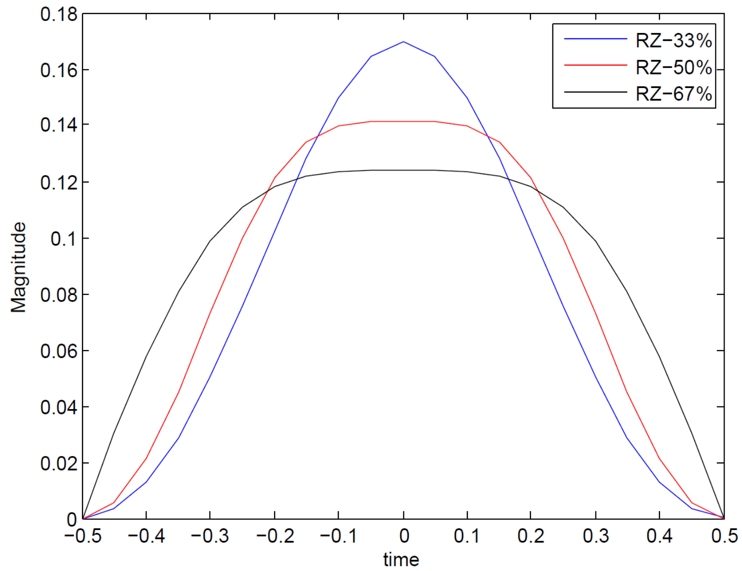

Figure 2.3: RZ pulse with different duty cycles.

2.2 Channel

After being filtered from the pulse shaper, the pulse is sent to the optical channel. In order to understand the effect of optical channel on the transmitted pulse, various channel impairments are modeled. These channel impairments limit the performance of the system and thereby increases the system's BER:

- Phase noise
- Frequency offset
- CD
- PMD

Channel impairments modeled in this evaluation setup are shown in figure 2.4.

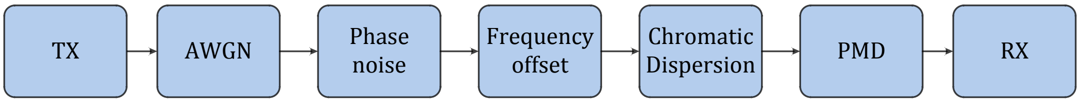

Figure 2.4: Channel.

2.2.1 Additive White Gaussian Noise (AWGN)

Additive white gaussian noise (AWGN) is modeled using the noise variance of a signal, σ_n. The noise variance of a signal, σ_n, is given by equation (2.4), where N_0 is the one side noise power spectral density and f_s is the sampling frequency.

$$\sigma_n = \frac{N_0 f_s}{2} \tag{2.4}$$

2.2.2 Phase Noise and Frequency Offset

Phase noise is caused by the lasers in the modulator. This noise is actually manifest in the modulator, and not in the channel. Phase noise is associated with the spontaneous emission that occurs during the operation of the laser. Basically, the light emitted by the laser is due to two types of emission, spontaneous and stimulated emission. The light amplified by the process of stimulated emission is in the same frequency and phase as the incoming light but due to spontaneous emission, there are random phase noise and frequency offset included in the system. This can be reduced by using lasers of very small line width.

If $\phi(t)$ is the phase of the signal which is transmitted, due to the phase noise $\Delta\phi(t)$ the phase of the signal at the receiver $\phi_r(t) = \phi(t) + \Delta\phi(t)$. This phase noise introduces a time varying phase and, therefore, causes a BER degradation in the receiver.

In this setup, the generated pulse is multiplied with $e^{j\phi}$, where ϕ is the random phase noise, whose variance is $\sigma_{phasenoise}$. Similarly, the frequency offset is obtained by multiplying the generated pulse with e^{jfreq} where $freq$ is given by $\theta_0 + \frac{2\pi k T_s}{T}$.

2.2.3 Chromatic Dispersion (CD)

Chromatic dispersion occurs in an optical transmission channel due to the dependence of group velocity and phase velocity on optical frequency [9]. The optical transmitting source is not monochromatic [10]. Considering these two facts it can be stated that different wavelengths tend to travel with different velocities, thereby causing pulse broadening.

The group delay (τ_g) of a spectral component, with angular frequency ω, fiber length z, is given by equation (2.5).

$$\tau_g = -z\frac{\lambda^2}{2\pi c}\frac{d\beta}{d\lambda} \tag{2.5}$$

where β is the propagation constant.
The group velocity's (ν_g) dependence on β is given by $\nu_g = (d\beta/d\omega)^{-1}$. The transfer function of the chromatic dispersion is given by equation (2.6).

$$H(\omega) = exp(\frac{j}{2}\beta_2\omega^2 z) \tag{2.6}$$

where $\beta_2 = \frac{d^2\beta}{d\omega^2}$ is the second order dispersion parameter.

There are basically two causes of chromatic dispersion, one is waveguide dispersion and the other is material dispersion. The material dispersion occurs due to the dependence of wavelength on the refractive index of the fiber core material, while the waveguide dispersion occurs because of the dependence of propagation constant on wavelength and fiber parameters like fiber core radius, difference in refractive indices in fiber core and cladding [10].

2.2.4 Polarization Mode Dispersion (PMD)

The simulations done in this thesis are only for single mode fiber. As its name implies, it allows only one mode of propagation but to transmit at higher rates, we can polarize signals and transmit them. In a perfect optical channel, if two different polarizations are transmitted, they travel at the same speed. The change of birefringence of the fiber affects the group velocity of the polarization thereby causing them to travel at different speeds [11]. This results in pulse distortion and affects the performance of the system. Polarization mode dispersion can be modeled by known fiber properties.

Jones vector and Jones matrix

The Jones vector represents the electric field of a signal in an optical fiber with two polarizations [10] and is given by equation (2.7).

$$E = \begin{pmatrix} E_x \\ E_y \end{pmatrix} = \begin{pmatrix} E_{0x}e^{j\delta_x} \\ E_{0y}e^{j\delta_y} \end{pmatrix} \tag{2.7}$$

- E_{0x}, E_{0y} - amplitude.
- δ_x, δ_y - phase.

The components E_x and E_y are complex quantities. The output electrical field (E') of an optical channel with polarization dispersion can be calculated from the input electric (E) field using the Jones matrix (J) [10].

$$E' = J \cdot E \tag{2.8}$$

The general form of the Jones matrix is given by equation (2.9). The Jones matrix is the impulse response of a polarization medium [10].

$$J = \begin{pmatrix} j_{xx} & j_{xy} \\ j_{yx} & j_{yy} \end{pmatrix} \tag{2.9}$$

Substituting suitable values for j_{xx}, j_{xy}, j_{yx}, and j_{yy}, jones matrix for linear or circular polarization can be obtained.

First order polarization mode dispersion

The transfer function of the polarization mode dispersion is given by equation (2.10)

$$H_{PMD}(t,\omega) = -e^{2j\omega\tau_{DGD}\frac{(t)}{2}} \begin{bmatrix} cos\theta(t) & -sin\theta(t)e^{-j\phi(t)} \\ sin\theta(t)e^{-j\phi(t)} & cos\theta(t) \end{bmatrix} \begin{bmatrix} cos\theta(t) & sin\theta(t)e^{-j\phi(t)} \\ -sin\theta(t)e^{-j\phi(t)} & cos\theta(t) \end{bmatrix} \tag{2.10}$$

- $\tau_{DGD}(t)$- Differential group delay
- $\theta(t)$- rotation.
- ϕ- Phase shift.

2.3 Receiver

The receiver used in this system test bench is a coherent receiver, that is, the receiver is aware of what data it is supposed to receive. Coherent detection allows the electronic processing of the received signal. Frequency and phase modulation is possible in coherent detection while it is not possible in direct detection.The Analog to Digital (A/D) conversion is considered to be perfect here. The effect of A/D conversion on the system is not considered, but the fixed point conversion effect is considered only before our block of interest. Anti aliasing is avoided using a low-pass anti-aliasing filter. The first block in the receiver is the chromatic dispersion compensation block, followed by the primary block of interest (that is, the STR block), the equalizer and the BER estimator.

The reference point is the input power when the BER is 10^{-3}. In optical systems, the input power is given in dBm. Furthermore, a lower input power is preferred for transmission, because the nonlinearities in the optical channel will increase proportionally with input power.

2.3.1 Chromatic Dispersion Filters

Chromatic dispersion increases the width of the transmitted optical pulse and causes inter symbol interference. For standard single-mode fibers driven by a directly modulated laser diode transmitter, the pulse spread due to chromatic dispersion is given by the dispersion parameter β_2[12].

There is one particular wavelength where the material and waveguide dispersion cancels each other and results in zero dispersion; that wavelength is located at 1330 nm and is called the zero dispersion wavelength. The wavelength at 1550 nm is said to have maximum dispersion and this is represented by λ in this thesis.

The chromatic dispersion parameter is given as $D = 17$ ps/nm/km. The group velocity dispersion parameter β_2, which is calculated from the dispersion parameter D using equation (2.11), has an approximative value of $-21 \cdot 10^{-22}$ ns^2/km. The transfer function used to implement the chromatic dispersion filter is given in equation (2.12). The time domain representation of the same function is given in equation (2.13).

$$\beta_2 = -\frac{D\lambda^2}{2\pi c} \tag{2.11}$$

$$U_F(z,\omega) = U_F(0,\omega)exp(\frac{j}{2}\beta_2\omega^2 z), \tag{2.12}$$

$$U(z,T) = U(0,T) \otimes \frac{1}{\sqrt{-2j\pi\beta_2 z}}exp(\frac{jt^2}{2\beta_2 z}) \tag{2.13}$$

The chromatic dispersion which occurs in the channel needs to be compensated in the receiver end. A solution for this CD compensation is by using FIR filters having the inverse transfer function of chromatic dispersion [12]. The coefficient for the filter is developed based on the length of the fiber. The number of filter coefficients needed for the generation is given by equation (2.14) and (2.15).

$$N = 2 \times \left\lfloor \frac{|D|\,\lambda^2 z}{2cT^2} \right\rfloor + 1 \tag{2.14}$$

The coefficients of the filtering operation are calculated using equation (2.15) [12]. The filter order depends upon the length of the fiber (z). An estimate of chip area of CD filters for a length of 100 km was found to be around 6336 μm^2. This area estimation of CD filters were obtained in a similar manner as area values obtained for STR block in the table 4.1.

$$a_k = \sqrt{\frac{jcT^2}{D\lambda^2 z}}exp(-jk^2\frac{\pi cT^2}{D\lambda^2 z}) \qquad where \left\lfloor -\frac{N}{2} \right\rfloor \leq \left\lfloor \frac{N}{2} \right\rfloor \tag{2.15}$$

2.4 Validation of Evaluation setup

The evaluation setup had to be validated before we could compare the results of different algorithms. The validation of the setup was mainly based on constellation plots and manual verification. Initially, the setup was tested without any noise. The expected constellation plot will be an unscattered constellation plot. The magnitude of the plot will be dependent on the input power and upon the estimated timing offset. Manually correct timing offset was provided to the timing estimation block, and it resulted in the exact constellation plot as input.

As the next step AWGN was added in the channel, and the BER curve was plotted. It was observed that at low input power from -100 dBm to -60 dBm the BER curve was flat and this phenomenon was expected, due to the decrease in signal power in comparison with noise power. Later other channel impairments were added, and they were verified using constellation plots.

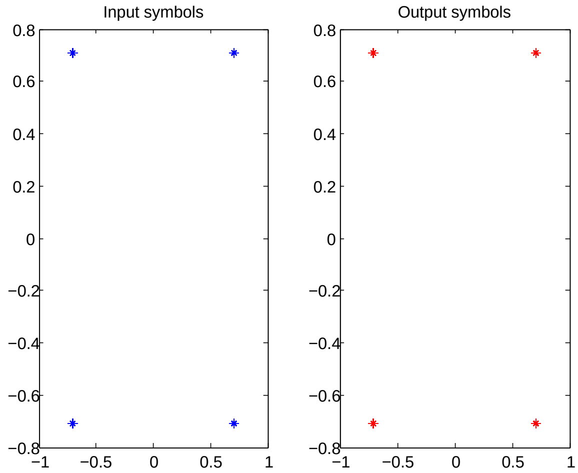

Figure 2.5: Constellation plot: System without noise and channel impairments

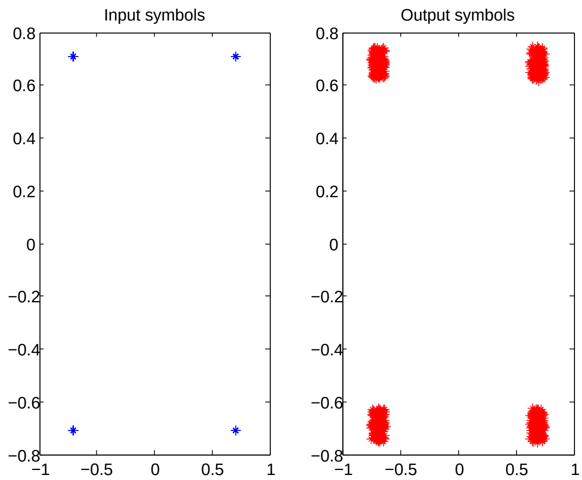

Figure 2.6: Constellation Plot: System with AWGN noise

3

Symbol Timing Recovery

Symbol timing recovery involves the estimation of the symbol period. The symbol period is a known quantity but due to the oscillator drift, the symbol timing will deviate from the known value. This deviation of symbol timing is denoted as timing offset (τ). Three different algorithms are modeled to estimate τ and this value is used in interpolation to recover the symbols.

The symbol timing recovery block is composed of three distinct subblocks:

- Matched filter.
- Timing offset estimation.
- Interpolation.

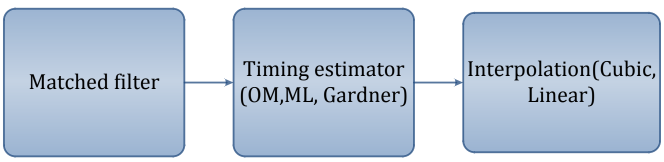

Figure 3.1: Symbol Timing Recovery

3.1 Matched Filter

In communication systems, there is a necessity to sample the signal at the correct instance. Before sampling the signal at the right instance, it is necessary to filter the signal. The sampling filter and the matched filter are popularly used filtering concepts, the latter comes with more advantages hence it is widely used. Matched filtering also filters out the unwanted frequency thereby improving the SNR.

The matched filter's impulse response is the reverse of the time shift version of the input pulse. The matched filter performs the convolution of the received signal with the reverse time shifted version of the input pulse. It correlates the received signal with the transmit pulse shape over the symbol period T.

- $p(t) - 0 \leq t \leq T$ transmitted pulse.
- $p(T-t) - 0 \leq t \leq T$ pulse response of ideal matched filter.
- y(t)= x(T)*p(T-t) output of matched filter

3.2 Timing Estimation

3.2.1 Maximum Likelihood (ML) Algorithm

The ML algorithm is a feedforward algorithm, and it works using the Maximum likelihood estimation principle. Equation (3.1) describes the likelihood function $\Lambda(\widehat{\tau})$. The Maximum likelihood estimator calculates the $\widehat{\tau}$ which maximizes equation (3.1).

$$\Lambda(\widehat{\tau}) = \sum \widehat{a}(n) m(n,\widehat{\tau}) \tag{3.1}$$

- $\widehat{a}(n)$ - correct symbol value.
- $m(n,\widehat{\tau})$ - samples from matched filter.
- $\widehat{\tau} \in (0,T)$ - timing error.

The ML algorithm requires at least two samples per symbol for $\widehat{\tau}$ estimation. The mathematical expression for the ML algorithm is written in equation (3.2) and the block diagram is shown in figure 3.2 .

$$\hat{\tau} = -\frac{T}{2\pi} arg \left\{ \sum_{k=ND}^{N(L+D)-1} x[(k-ND)T_s]\, e^{-\frac{j\pi(k-ND)}{N}} z[(k-ND)T_s] \right\} \tag{3.2}$$

where

$$z(kT_s) = \left[x^*\,(k_2 T_s)\, e^{-\frac{j\pi k_2}{N}} \right] \otimes q(kT_s) \tag{3.3}$$

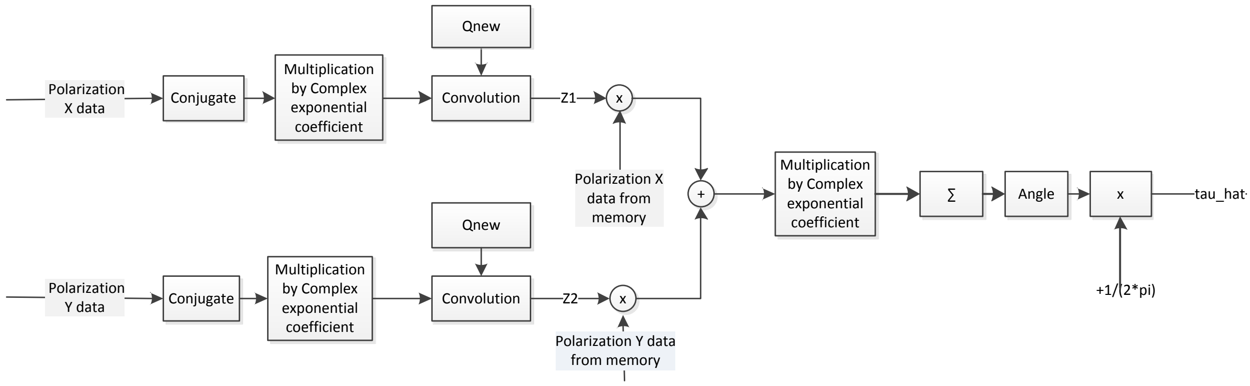

Figure 3.2: ML Block Diagram

and $q(t)$ is the Inverse Fourier Transform (IFT).

$$Q(f) = G\left(f - \frac{1}{2T}\right) G^*\left(f + \frac{1}{2T}\right) \tag{3.4}$$

- G(f) - Fourier transform of the used pulse g(t)
- L - length of trial signal (symbols)
- T - symbol period
- T_s - sampling period
- N - oversampling ratio (T/T_s)

3.2.2 Oerder & Meyr (OM) Algorithm

The Oerder & Meyr (OM) is a feedforward algorithm. Feedforward algorithms are relatively speaking faster than feedback algorithms in performing timing estimation [13]. The OM algorithm needs at least four samples per symbol for proper operation. Its mathematical expression is given in equation (3.5) and the block diagram is shown in figure 3.4.

$$\hat{\tau} = -\frac{T}{2\pi} arg\left\{\sum_{k=0}^{NL_0-1} |x(kTs)|^2 \, e^{-j2\pi k/n}\right\} \tag{3.5}$$

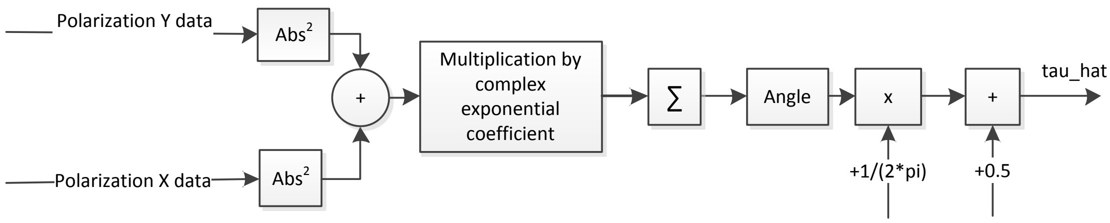

Figure 3.3: OM Block Diagram

3.2.3 Gardner Algorithm

The Gardner algorithm works using the feedback principle. Since it is a feedback algorithm, it is carrier insensitive. Figure 3.4 shows the block diagram of this feedback algorithm. The timing error detector (TED) estimates the timing error information from the received signal. The error signal $e(k)$ is filtered through a loop filter [14]. The error signal $e(k)$ is proportional to the difference between the actual timing offset τ and the estimated timing offset $\widehat{\tau}$. The timing corrector corrects the sampling time using the timing error estimation $e(k)$. The mathematical expression for the timing error estimation used in the Gardner algorithm is given in equation (3.6).

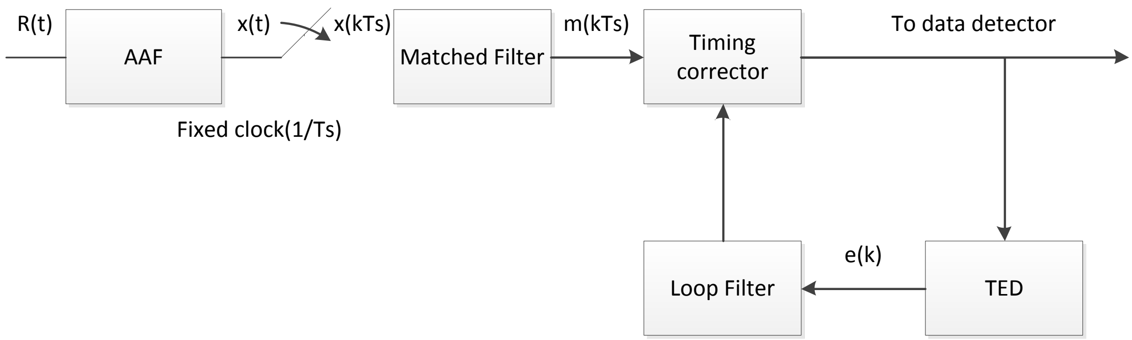

Figure 3.4: Feedback Block diagram

$$e(k) = Re\left\{r(kT - T + \hat{\tau}_{k-1}) - r(kT + \hat{\tau}_{k-1}) \times r^*(kT - \frac{T}{2} + \tau_{k-1})\right\} \tag{3.6}$$

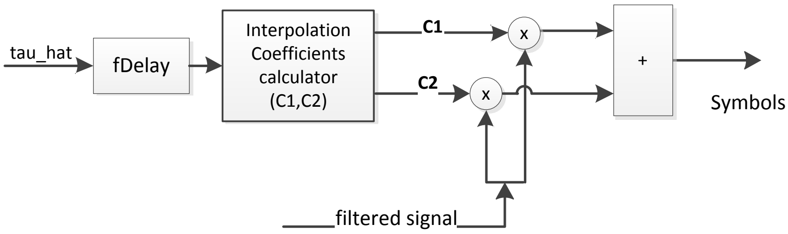

Figure 3.5: Linear Interpolation Block

3.3 Interpolator

The interpolator calculates the output samples using the $\widehat{\tau}$ calculated from the timing error detector. The interpolator selects the sample at the right sampling instance from the samples obtained after the matched filtering. The correct sampling instances(nT_i) is given by $nT_i = kT_s + \tau T_s$. The sample at these sampling instance $y(nT_i)$ would be the correct output sample. Two variations of interpolators, cubic and linear interpolator, were used in this project. The function of the interpolation is to calculate one output sample $y(nT_i)$ at a time, using a set of adjacent input samples m(kT) and the timing error estimate is obtained from the timing estimator.

3.3.1 Linear Interpolation

The interpolation block takes the timing error information and the incoming samples, corrects the timing error and downsamples into one symbol. The coefficients for linear interpolation are given below:

$$C1 = u \tag{3.7a}$$
$$C2 = 1 - u \tag{3.7b}$$

The block diagram of a linear interpolator is shown in figure 3.5.

3.3.2 Cubic Interpolation

The coefficients for cubic interpolation are given below.

$$C1 = u^3/6 - u/6 \tag{3.8a}$$
$$C2 = -u^3/2 + u^2/2 + u \tag{3.8b}$$
$$C3 = u^3/2 - u^2 - u/2 + 1 \tag{3.8c}$$
$$C4 = -u^3/6 + u^2/2 - u/3 \tag{3.8d}$$

where u is rem($\hat{\tau}$,1) from the symbol timing recovery algorithms.

The block diagram of the cubic interpolation block is shown in figure 3.6.

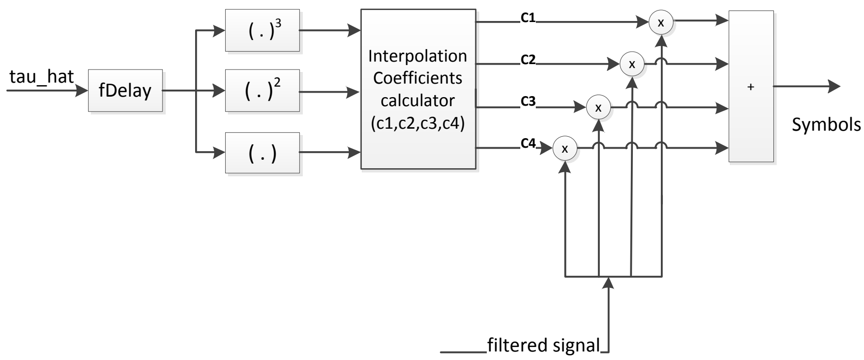

Figure 3.6: Cubic Interpolation Block

4

System Analysis and Word Length Optimization

4.1 Fixed Point Conversion

In order to develop an algorithm in hardware, the word length required by each subblock of the STR circuit must be established. The MATLAB fixed point tool was used to find the minimum word length for various blocks. The MATLAB 'fimath' properties used for this thesis are shown below.

- Overflow mode: Saturate
- Sum mode: Keep MSB
- Product mode: Keep MSB

The degradation of BER when we decrease word length is shown in figure 4.8 and 4.9. The area and power estimation of the STR block using the minimum word length is shown in table 4.1.

The Maximum likelihood (ML), Oerder and Meyr (OM) and Gardner algorithms were evaluated using the evaluation setup developed. The parameters used to compare the performance of these algorithms are BER and timing estimation error. The OM algorithm requires 4 samples/symbol, while the ML algorithm and Gardner can work with 2 samples/symbol. Otherwise, all three algorithms were evaluated for the same specification. The bit rate calculation is given below.

- Baud rate: 28 Gbaud
- Constellation: QPSK

- No. of polarizations: 2
- No. of bits per symbol: 2

$$Bitrate = Baudrate \times No.ofPolarization \times No.ofbitspersymbol. \tag{4.1a}$$
$$= 28 \times 10^9 \times 2 \times 2. \tag{4.1b}$$
$$= 112Gbits/sec. \tag{4.1c}$$

Table 4.1: Area and power for STR algorithms with different interpolators

Algorithm	Interpolator	Clock rate:500 MHz		Clock rate: 2 GHz	
		Area(μm^2)	Power(mW)	Area(μm^2)	Power(mW)
OM	Cubic	604966	96.27	224275	55.18
ML	Cubic	654385	111.71	327670	88.97
Gardner	Cubic	604478	102.75	210673	60.45
OM	Linear	288460	47.90	116465	28.90
ML	Linear	337879	61.98	206780	62.69
Gardner	Linear	276502	50.38	99073	30.24

4.2 Effect of Channel Impairments on STR

The main purpose of this evaluation is to compare different STR algorithms. As mentioned earlier OM algorithm will need at least 4 samples/symbol, while ML and Gardner can work with 2 samples/symbol. OM is a simplified version of ML.

4.2.1 AWGN

Figure 4.1 shows the BER curve for three different algorithms. The ideal one represents when the timing estimate is perfect. It should not be misunderstood from the plot that ML has lower performance than OM. The reasons behind these curves are the algorithms were simulated for their minimum requirement. ML was made to run with 2 samples/symbol while OM was made to run with 4 samples/symbol. The reason behind this choice is the area and power requirement for hardware implementation of ML will increase as the number of samples increases. This could be understood from the area values in table 4.1.

On the other hand, being a feedback algorithm, Gardner's algorithm is expected to have much better performance than the feedforward ones. It could have been true if the timing offsets varies rapidly, which is not the case in the optical communication system. All these above reasons make the performance of all these algorithms more or less similar.

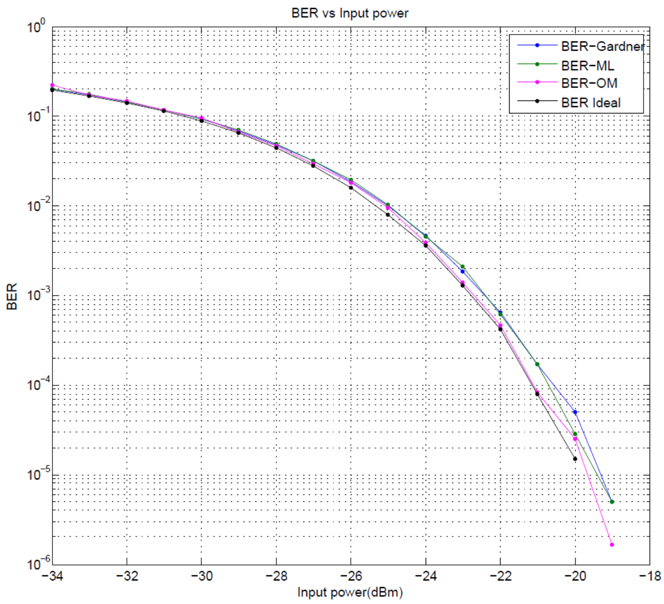

Figure 4.1: BER comparison curve (white noise)

4.2.2 Phase Noise

Figure 4.2 shows the BER curve plotted against input power (dBm) in the presence of phase noise. Since we aimed at analyzing just the symbol timing estimate of the system, we made the phase noise recovery at the receiver side to be perfect. Thereby the variation in BER would be purely because of timing estimation. As a reader one can look at the power required to obtain a BER of 10^{-3}. Unlike the previous plot, there is a difference in performance between OM and other algorithms. If ML is simulated with the same number of samples/symbol as OM, ML results in better results.

4.2.3 Frequency Offset

Figure 4.3 shows the BER curve plotted against input power (dBm) in the presence of frequency offset.

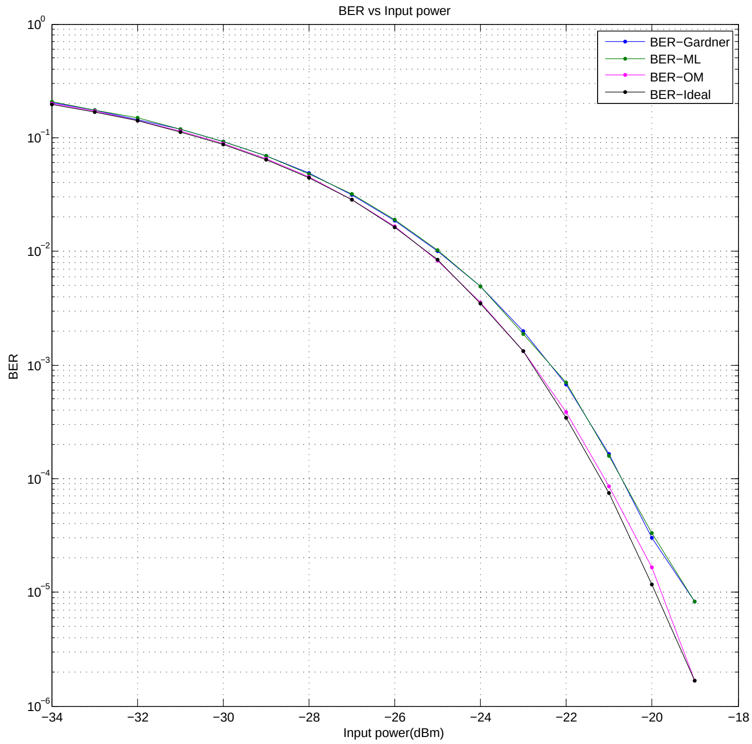

Figure 4.2: BER comparison curve (phase noise)

4.2.4 Chromatic Dispersion

Figure 4.4 shows the comparison plot for ML, OM and Gardner's algorithm in the presence of chromatic dispersion.

4.2.5 Comparison

Figure 4.5 shows the comparison plot for ML, OM and Gardner's algorithm in the presence of AWGN, phase noise, frequency offsets and chromatic dispersion.

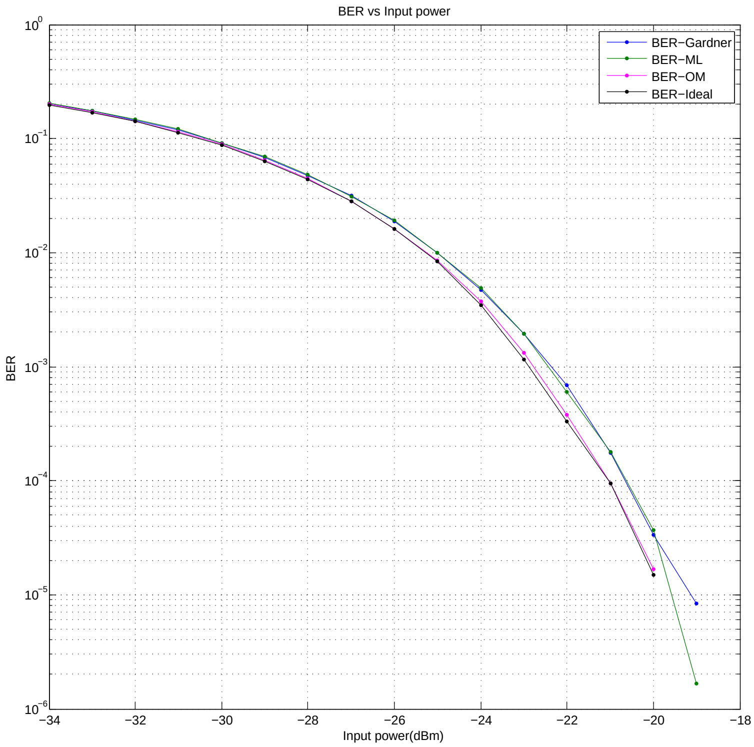

Figure 4.3: BER comparison curve (frequency offset)

In hardware, there is limitation in clock rate at which data can be processed [2]. Parallelization of stages is required to process the data at the required rate, assuming the clock rate is lower than the required rate. Parallelization has a direct impact on the area and power consumption of the hardware. Power dissipation is one key design parameter when it comes to hardware implementation of any algorithm. Before an algorithm can be implemented in hardware, various trade-offs are required to be analyzed.

Symbol timing recovery comprises two blocks, that is, the timing estimator and the interpolation block. If we use all the incoming samples to estimate the timing offset, the timing estimator will occupy more hardware. In optical systems, the timing offset

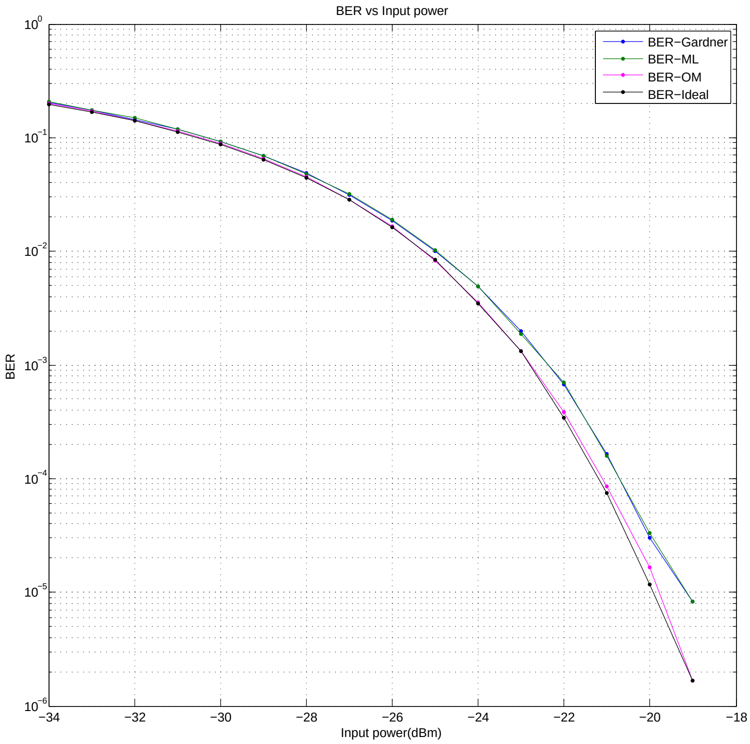

Figure 4.4: BER comparison curve (chromatic dispersion).

varies very slowly. Thus, it is possible to find out a minimal number of samples that are required to estimate the timing offset. Simulations were performed to find the minimum number of samples required for hardware implementation [1].

On the other hand, the interpolation block (figure 3.6) needs to be operated at high speed, and it needs data to be pipelined, thereby leaving less room for optimizations [2]. The area consumption of the interpolation block was found to be 10 times higher than the timing estimator block (table 4.1). The initial interpolation block used was cubic interpolation, which required four multiplications (figure 3.6) for each parallel stage. If the number of multiplications were reduced, less hardware is required. Subsequently, linear interpolation was tried out to reduce the number of multiplications (figure 3.5).

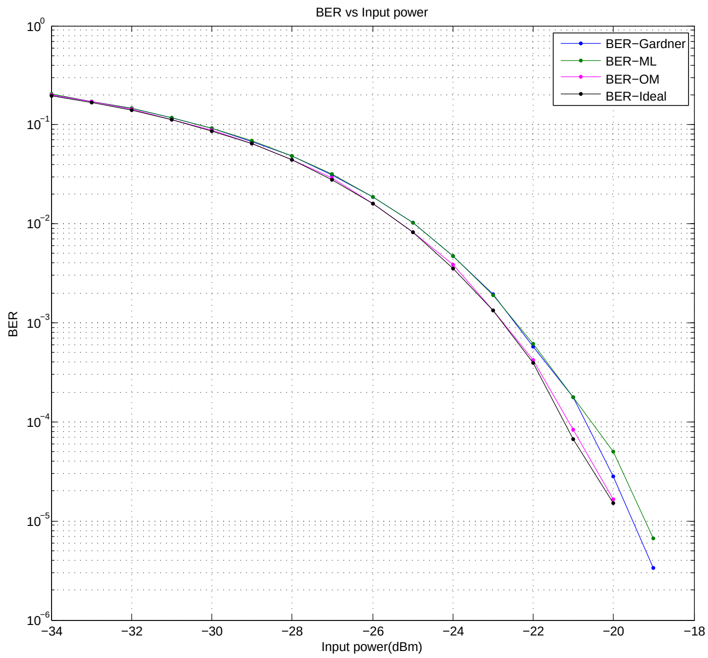

Figure 4.5: BER comparison curve.

4.3 Wordlength versus BER

The hardware implementation of the STR algorithms showed that the area occupied by the timing estimator is far less than for interpolation [2]. The area occupied by the interpolator and the timing estimator depends greatly upon the word length of the subblocks. In an approach to understand the impact of word length on area, BER values were plotted against various word lengths. The factor w was assigned as a scaling factor for the timing estimator block and a factor i was assigned for interpolation blocks. Figure 4.6 and 4.7 shows the blocks with scaling factor w and i, respectively. Simulation results showed that the minimum value for w and i is 3 and 6 bits, respectively. The plots in figure 4.8 and 4.9 show the relation of word length to BER and timing estimation. The x-axis was plotted for the scaling factor. The BER value and the difference in τ estimations between floating to fixed-point version of the algorithm were plotted on the y-axis. The choice of word length depends upon on our requirement of performance.

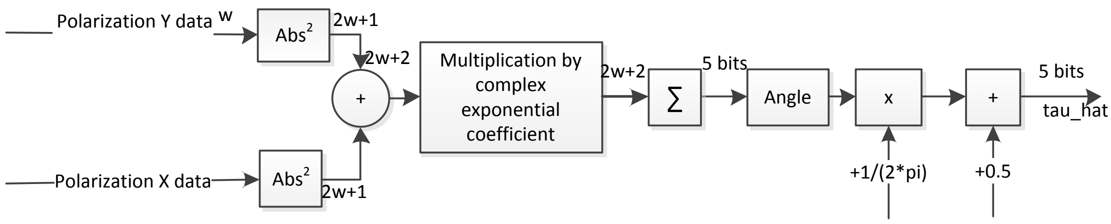

Figure 4.6: Word length scaling (timing estimation)

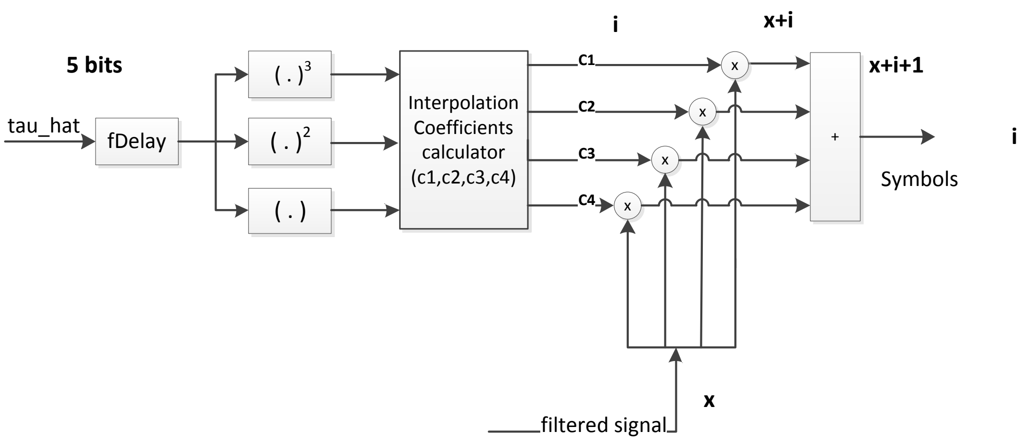

Figure 4.7: Word length scaling (interpolation)

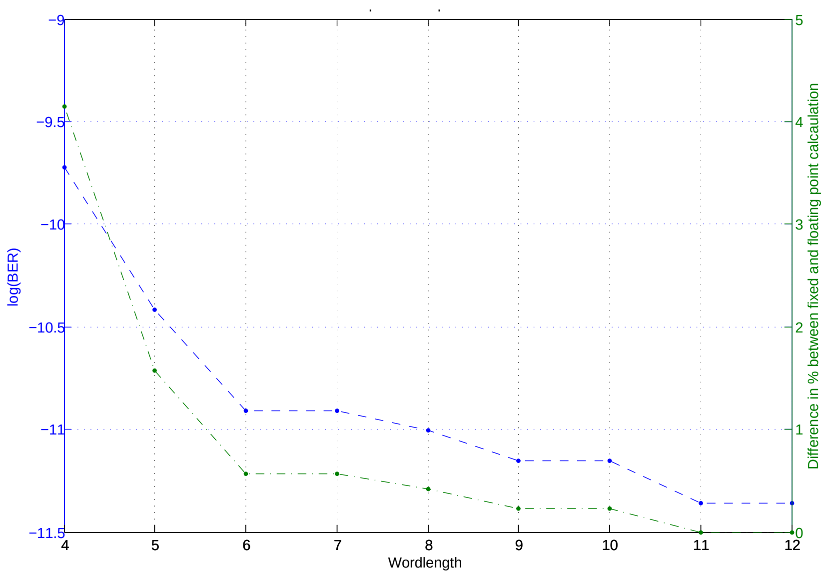

Figure 4.8: Word length effect on BER (timing estimator block)

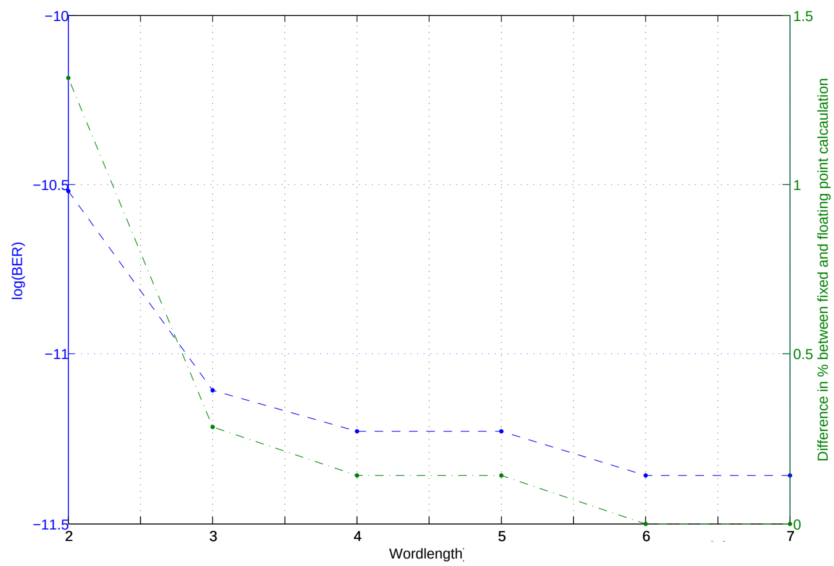

Figure 4.9: Word length effect on BER (interpolation block)

5

Discussion and Conclusion

The symbol timing recovery can be performed by using either feedforward or feedback algorithms. Feedback algorithms are robust against fast fluctuations in the timing offset [15]. The feedforward ML algorithm architecture is more complex than the feedback algorithm. Oerder and Meyr developed a feedforward algorithm, the OM algorithm, which is a variation of the ML algorithm [13]. In the first place, we compared feedforward algorithms. The ML has a higher hardware complexity and better performance than the OM algorithm. The complexity of ML results in a very high area requirement and for this reason the ML algorithm was evaluated for its minimum requirement of 2 samples/symbol. In that situation results showed than OM performs better than ML. In circumstances where timing estimation is not a critical factor it is wise to choose the OM algorithm, which would give marginally lower performance than ML with the advantage of low area and power.

Now the choice is narrowed down to OM and the Gardner algorithm [16]. The Gardner algorithm occupies less area compared to OM but due to the presence of the feedback loop it requires more power than OM. Thus, the OM algorithm will be a good choice for a power-efficient system. Although various channel impairments were analyzed, the nonlinear effect was not studied in this thesis, which means that the effect of transmitter/channel nonlinearities on the STR block is still unknown. The estimate of CD filters provided is approximate. The order of the FIR filter increases linearly with the increase in fiber length. There exist various research works for the optimization of CD filters [17] [18]. In this thesis QPSK modulation was used along with two polarizations to achieve a bit rate of 112 Gbits/sec. Beyond 112-Gbits/sec transmission, additional technology will be necessary to overcome the degradation of bit error rate [19]. For this purpose forward error correction (FEC) can be performed. FEC can suppress the transmission penalty due to CD and PMD, thereby reducing the BER [19].

Bibliography

[1] Y. Ai, Clock Recovery for High-Speed Fiber-Optic Communication Systems, Master's thesis (Jun. 2012).

[2] T. Ahmad, Implementation and Optimization of High-Speed Symbol Timing Recovery Algorithms, Master's thesis (Jun. 2012).

[3] A. Rhodin, J. Mårtensson, SCM System Analysis: Part 6 - DSP sub-system (2010).

[4] U.-V. Koc, Adaptive Electronic Dispersion Compensator for Chromatic and Polarization-Mode Dispersions in Optical Communication Systems, EURASIP Journal on Applied Signal Processing (2004) 1584–1592.

[5] N. I. tutorial, Fpga fundamentals (May 2012).
URL `http://www.ni.com/white-paper/6983/en`

[6] I. Kuon, J. Rose, Measuring the Gap Between FPGAs and ASICs, IEEE Transactions on Computer-Aided Design of Integrated Circuits and Systems 26 (2) (2007) 203 –215.

[7] F. Toft, N. Rousk, Real-Time Signal Processing Implementation for 100 Gb/s Fiber Communication, Master's thesis (Jul. 2011).

[8] E. Ip, J. M. Kahn, Power Spectra of Return-to-Zero Optical Signals, Journal of Lightwave Technology 24 (3) (2006) 1611.

[9] M. Khafaji, H. Gustat, F. Ellinger, C. Scheyt, General Time-Domain Representation of Chromatic Dispersion in Single-Mode Fibers, IEEE Photonics Technology Letters 22 (5) (2010) 314–315.

[10] W. Shieh, I. Djordjevic, OFDM for Optical Communications, Academic Press, 2010.

[11] J. P. Gordon, H. Kogelnik, PMD fundamentals: Polarization mode dispersion in optical fibers, Proceedings of the National Academy of Sciences of the United States of America 97 (9) (2000) 4541–4550.

[12] S. J. Savory, G. Gavioli, R. I. Killey, P. Bayvel, Electronic compensation of chromatic dispersion using a digital coherent receiver, Optics Express 15 (5) (2007) 2120–2126.

[13] M. Oerder, H. Meyr, Digital filter and square timing recovery, IEEE Transactions on Communications 36 (5) (1989) 605–612.

[14] F. Gardner, A BPSK/QPSK Timing-Error Detector for Sampled Receivers, IEEE Transactions on Communications 35 (5) (1986) 423–429.

[15] D. Schmidt, B. Lankl, Structure of a Digital Feedback Clock Recovery for Parallelized Receivers, in: Signal Processing in Photonic Communications, Optical Society of America, 2011, p. SPTuC2.

[16] D. Zibar, J. C. R. F. de Olivera, V. B. Ribeiro, A. Paradisi, J. C. Diniz, K. J. Larsen, I. T. Monroy, Experimental investigation and digital compensation of DGD for 112 Gb/s PDM-QPSK clock recovery, Optics Express 19 (26) (2011) B429–B439.

[17] B. S. G. Pillai, B. Sedighi, W. Shieh, R. S. Tucker, Chromatic Dispersion Compensation - An Energy Consumption Perspective, in: Optical Fiber Communication Conference, Optical Society of America, 2012, p. OM3A.8.

[18] E. Ip, J. M. Kahn, Compensation of Dispersion and Nonlinear Impairments Using Digital Backpropagation, Journal of Lightwave Technology 26 (20) (2008) 3416–3425.

[19] E. Yamazaki, M. Tomizawa, Y. Miyamoto, 100-Gb/s Optical Transport Network and Beyond Employing Digital Signal Processing, IEEE Communications Magazine 50 (2) (2012) s43–s49.